ELSEVIER

Etching of uranium oxide with a non-thermal, atmospheric pressure plasma

X. Yang [a], M. Moravej [a], S.E. Babayan [b], G.R. Nowling [a], R.F. Hicks [a,*]

[a] *Department of Chemical Engineering, University of California (UCLA), 405 Hilgard Avenue, Los Angeles, CA 90095-1592, USA*
[b] *Surfx Technologies LLC, 10624 Rochester Avenue, Los Angeles, CA 90024, USA*

Abstract

The etching of uranium oxide films was investigated with a non-thermal, atmospheric pressure plasma fed with a mixture of 2.0 kPa carbon tetrafluoride, 880.0 Pa oxygen and 97.2 kPa helium. Etching rates of up to 4.0 μm/min were recorded at a 200 °C sample temperature. X-ray photoemission spectroscopy revealed that the etched surface was highly fluorinated, containing UOF_4 species during the etching process. An average surface reaction rate was estimated to be 1.9×10^{19} UF_6 molecules/m^2 s.
© 2003 Elsevier B.V. All rights reserved.

1. Introduction

The production of nuclear weapons and fuel-grade uranium has left a large number of facilities contaminated with radioactive material throughout the United States. The cost of decontaminating and decommissioning (D&D) these facilities has been estimated to be up to $200 billion dollars by the Department of Energy [1,2]. In the meantime, there is increasing concern of dispersing radioactive materials from contaminated buildings and equipment into the environment. New technologies are of great interest for accelerating the clean up effort. Especially if these technologies can decontaminate the surfaces of glove boxes and other equipment so that they may be reclassified from transuranic waste to low-level radioactive waste.

Plasma etching, a process widely used in the fabrication of microelectronic devices, is being explored as a means to remove transuranic waste from contaminated sites. Martz et al. [3] first demonstrated the possibility of removing plutonium with a radio frequency, CF_4–O_2 plasma at low pressure. Recently, Veilleux et al. [4] and Kim et al. [5] have investigated the etching of uranium dioxide by CF_4–O_2 and NF_3 plasmas at low pressure. Etching rates of radioactive materials were found to range between 0.2 and 7.0 μm/min. Windarto et al. [6] have examined the decontamination using CF_4–O_2 microwave plasma torch at atmospheric pressure. One of the advantages of using atmospheric pressure plasmas is that it does not require the contaminated objects to be inserted into a vacuum chamber.

Hicks and coworkers [7–11] have shown that stable, capacitive discharges may be produced at atmospheric pressure by feeding helium between two electrodes driven with radio frequency power (e.g., 13.56 MHz). This discharge differs from other atmospheric pressure plasmas, such as torches, dielectric barrier discharges, coronas and cold cathodes, in that the neutral gas temperature is below 200 °C and the weakly ionized gas is homogeneous in space and time [7]. For the decontamination application, this device may be fed with CF_4 and O_2. Reactive species generated in the plasma will react with the radioactive elements, and convert them into volatile metal fluorides. For example, it has been shown that the CF_4–O_2 plasma etches tantalum, a surrogate for plutonium, at rates up to 6.0 μm/min at 1 atm and 300 °C [11].

---

* Corresponding author. Tel.: +1-310 206 6865; fax: +1-310 206 4107.

  E-mail address: rhicks@ucla.edu (R.F. Hicks).

In this article, we report on the etching of uranium oxide films with the non-thermal, atmospheric pressure plasma. The film surfaces have been examined by X-ray photoelectron spectroscopy and scanning electron microscopy. Relatively high etch rates are observed, demonstrating the viability of this approach for D&D applications.

2. Experimental methods

Uranium dioxide test samples were prepared by applying a 100 µl solution of uranyl nitrate hexahydrate (Strem Chemicals, Cat. 93-9212) with a concentration of 5 mg(uranium)/ml on 1×2 cm^2 stainless steel coupons. These samples were dried in air, and then baked for 5 h at 700 °C. This decomposed the uranyl nitrate to form a black spot of uranium oxide on the stainless steel surface. Each sample contained about 0.5 mg of uranium.

The apparatus used in these experiments has been described previously [11]. A schematic of the plasma source is shown in Fig. 1. It consisted of two concentric electrodes made of aluminum 15.0 cm in length and separated by a gap 1.6 mm across. The inner electrode measuring 1.27 cm in diameter was connected to an RF power supply (13.56 MHz). The outer electrode was grounded and equipped with a cooling jacket through which water flowed at 20 °C. Carbon tetrafluoride and oxygen were added to helium and the mixture passed through the annular space between the electrodes, where it was converted into a plasma. The partially ionized gas exited though a nozzle 4.9 mm in diameter at a linear velocity of 37 m/s (at 22 °C and 1 atm). After contacting the sample, the gas exhaust was bubbled through water to decompose the uranium hexafluoride reaction product.

The stainless steel coupon was placed on a stage located 3 mm downstream of the plasma and perpendicular to the gas flow. The stage contained a 250 W cartridge heater and a thermocouple that were connected to a temperature controller. The process conditions used to etch the UO_2 films were 880.0 Pa O_2, 2.0 kPa CF_4, 97.2 kPa He, 300 W RF power and a substrate temperature of 200 °C.

The morphology of the film surfaces was investigated before and after etching by scanning electron microscopy (Hitachi SEM, Model S-4700). The accelerating voltage ranged from 3.0 to 5.0 kV, and the operating distance was 5.4 ± 0.2 mm. The surface composition of the films was analyzed with a PHI 5000 X-ray photoelectron spectrometer (XPS), equipped with a hemispherical analyzer and a multichannel detector. Spectra were recorded at a take-off angle of 52° with respect to the sample normal using Al K_α X-ray and a pass energy of 23.5 eV.

3. Results

Shown in Fig. 2 are photographs of the stainless steel coupons before UO_2 deposition, after UO_2 deposition, after plasma etching, and after polishing the etched surface. Initially, the stainless steel coupon has a shiny metallic color. Uranium oxide deposition produces a black spot 0.7 cm in diameter with an average thickness of 20 µm (determined with a Veeco Dektak 8 profilometer). This UO_2 coating is completely stripped away following 5 min exposure to the fluorine plasma. Finally, the brown tarnish remaining after etching is easily removed with metal polish. An average etching rate of 4.0 µm/min is recorded at 200 °C and at the standard process conditions listed above.

In Fig. 3, scanning electron micrographs are presented of the uranium oxide films before plasma etching, and after etching for 2 and 5 min. The unprocessed film is porous with thin layers of material overlapping each other. Following 2 min of processing, the film is reduced to small aggregates 100–500 nm in length. This result shows that the reactive gas-phase species penetrate into the layers, and strip the uranium from all the exposed surfaces. After 5 min of treatment, the porous film is removed, leaving behind a roughed steel surface.
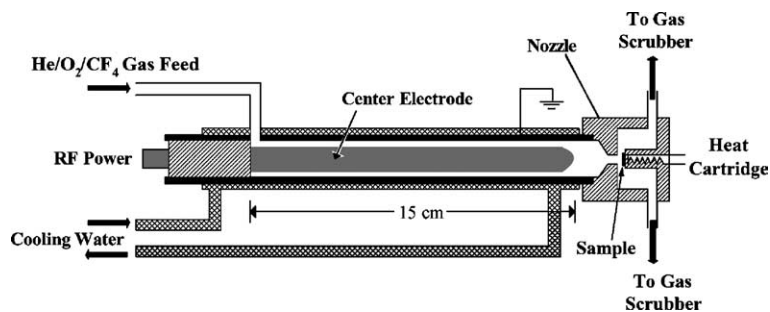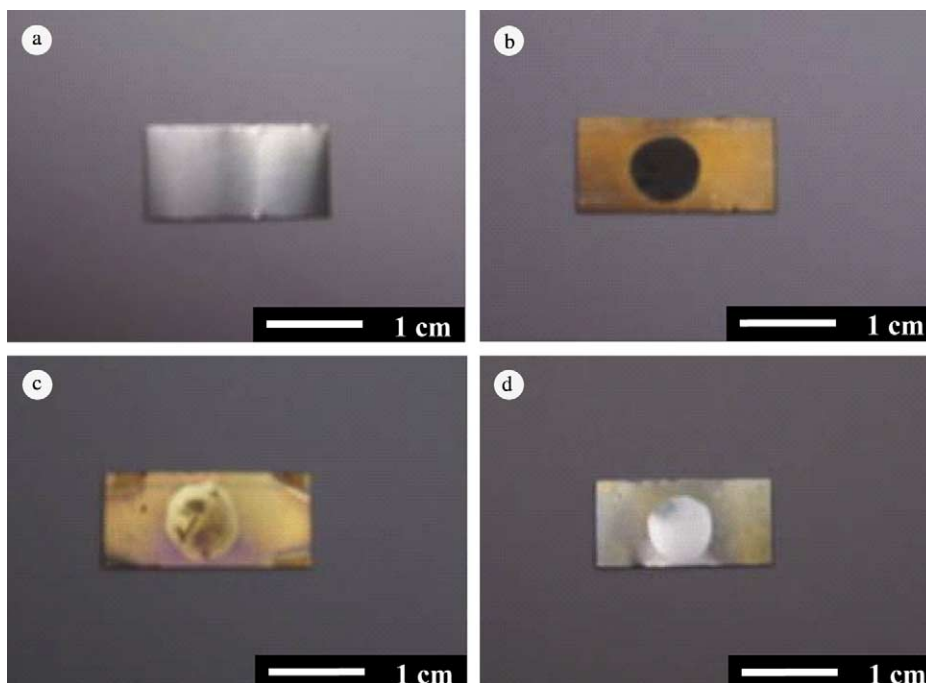

Fig. 1. Schematic of the experimental apparatus.

Fig. 2. Photographs of (a) the stainless steel coupon, (b) the uranium oxide film, 20 μm thick, (c) uranium oxide film is completely removed after etching for 5 min, and (d) the brown tarnish produced by the plasma treatment is easily removed with metal polish.

X-ray photoemission spectra of the UO_2 film before and after plasma etching for 2 min are shown in Fig. 4. Before exposure, one observes peaks at 284.0 eV due to the carbon 1s line, at 975.5 and 530.0 eV due to the oxygen Auger and 1s line, and at 783.0, 740.5, 391.7, 380.8, and 95.5 eV due to uranium $4d_{3/2}$, $4d_{5/2}$, $4f_{5/2}$, $4f_{7/2}$, and 5d photoemission, respectively [12]. The spectrum of the etched sample contains additional peaks at 835.1 and 687.5 eV due to the fluorine Auger and 1s lines, and at 714.5 and 645.0 eV due to iron 2p and nickel Auger peaks. Moreover, the U 4f emission intensity is much smaller than that recorded before etching.

The XPS analysis indicates that before etching, the sample surface is covered with UO_2, whereas after etching, this material has been heavily fluorinated. Moreover, plasma exposure has stripped uranium from the substrate surface, as evidenced by the dramatic decrease in intensity of the U 4f peaks, and the appearance of Fe and Ni photoemission from the stainless steel substrate. Also note that the intensity of carbon 1s peak does not change with plasma treatment, which indicates that no appreciable amount of fluorocarbon polymer is deposited on the sample from the $CF_4/O_2/He$ plasma effluent.

Shown in Fig. 5 are X-ray photoemission spectra of the U $4f_{5/2}$ and $4f_{7/2}$ states before and after etching the uranium oxide film. The U $4f_{7/2}$ peak for the fresh

sample has a binding energy of 380.8 eV, which is indicative of the U^{4+} oxidation state (UO_2). After exposure to the plasma for 1 min, the 4f peaks shift more than 3.0 eV to higher binding energy due to uranium oxidation to U^{6+}. The intensities of photoemission peaks decrease rapidly with treatment, so that after 5 min, essentially all of the uranium has been removed. A plot of the integrated intensity of the U $4f_{7/2}$ band with process time is shown in Fig. 6. Over the first minute, the intensity increases because the etching process initially increases the exposed surface area of the film (cf. Fig. 3). Then the intensity rapidly decays as the UO_2 particles are stripped away.

Presented in Fig. 7 are deconvoluted U $4f_{7/2}$ photoemission spectra obtained after etching 2 min at 100 and 200 °C. These spectra are composed of three overlapping bands due to the presence of different U^{n+} oxidation states. Initially, one peak at 380.8 eV is observed due to UO_2. Upon exposure to the fluorine plasma, this peak disappears and is replaced by the three bands at 381.6, 383.3, and 386.0 eV. The lowest energy state is assigned to uranium oxyfluoride (UOF_2) with 4+ valence, while the peaks at 383.3 and 386.0 eV are assigned to uranium oxyfluorides with 6+ valence, i.e., UO_2F_2 and UOF_4, respectively [5,12].

The distribution of the uranium among the different chemical states is shown in Table 1. These percentages have been calculated by taking the ratio of the area under
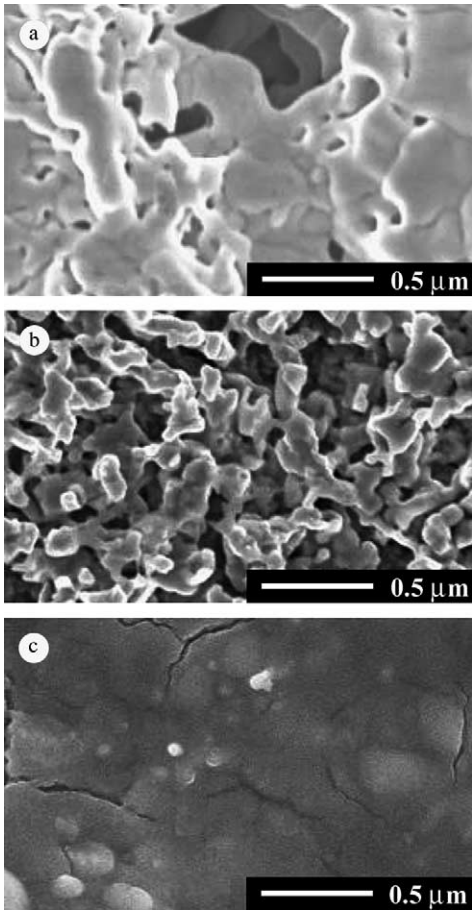
Fig. 3. Scanning electron micrographs of (a) UO₂ film before etching, (b) UO₂ film after a 2-min plasma etch, and (c) UO₂ film after a 5-min plasma etch.
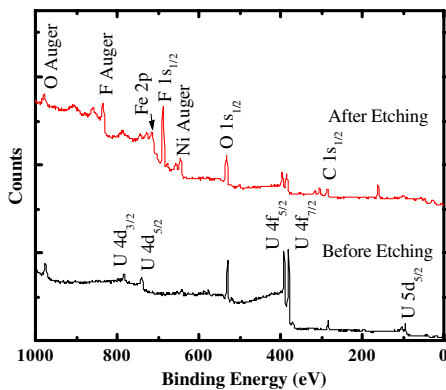

Fig. 4. X-ray photoemission spectra of UO₂ before and after a 2-min plasma etch.

a particular 4f$_{7/2}$ band to that under all the 4f$_{7/2}$ bands. It is found that UO$_2$F$_2$ is the dominant surface species
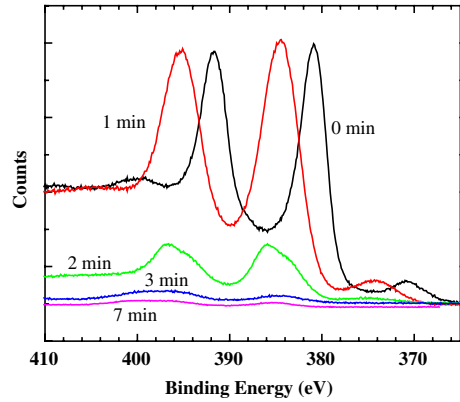

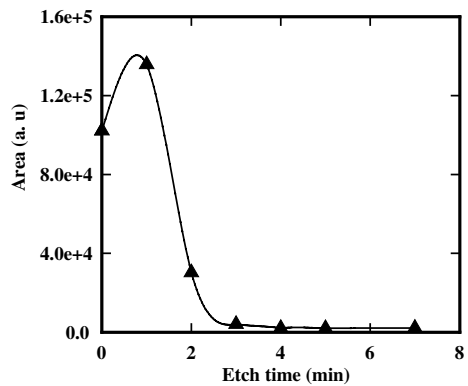Fig. 5. Uranium 4f photoemission spectra of UO₂ film before and after plasma etching.

Fig. 6. Integrated intensity of the U 4f$_{7/2}$ peak as a function of process time.

following plasma etching at 100 °C. On the other hand, UOF$_4$ constitutes 71% of the surface uranium at 200 °C. The formation of UO$_2$F$_2$ has been observed after etching UO$_2$ in a low-pressure CF$_4$/O$_2$ plasma, and in UO$_2$ fluorination with F$_2$ [5,13]. The more heavily fluorinated species at 386.0 eV has not been observed previously. The etching rate at 200 °C is two times faster than the etching rate at 100 °C. Evidently, surface intermediates play an important role in the etching process.

4. Discussion

To allow our results to be compared to other actinide etching studies, the surface reaction rate, R_s, may be estimated from the following equation:

$$R_s = \left(\frac{vA\rho}{M_{UO_2}} N_a \right) \frac{1}{S} \ (\text{molecules/m}^2 \, \text{s}), \tag{1}$$

where ρ is the density of amorphous UO$_2$ (4.8 g/cm^3) [4], N_a is Avogadro's number, M_{UO_2} is the molecular weight
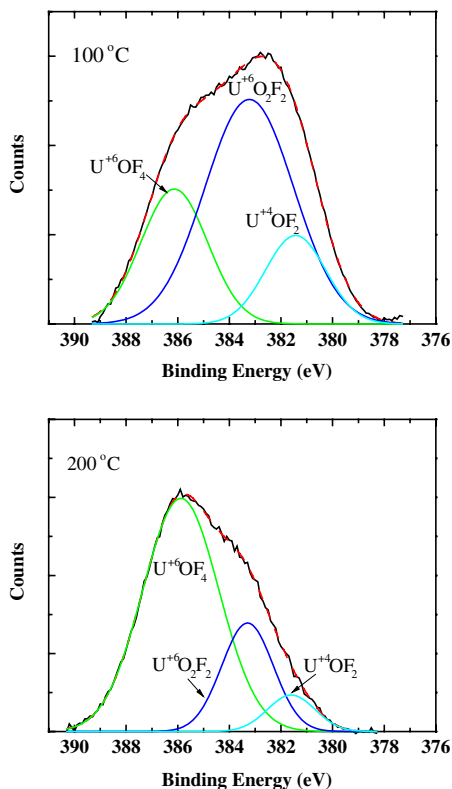
Fig. 7. Deconvolution of U $4f_{7/2}$ peaks after a 2-min etch at 100 and 200 °C.

Table 1
Percentage of uranium that is contained within each chemical state

State	Etching at 100 °C	Etching at 200 °C
UOF_2 (381.6 eV)	15.6	6.9
UO_2F_2 (383.3 eV)	58.3	22.3
UOF_4 (386.0 eV)	26.1	70.8
Total	100.0	100.0

of UO_2 (270.03 g/mol), v is the etch rate (µm/min), A is the area of the sample, and S is the total surface area of the film. Based on the SEM image taken after 2 min of etching, the film may be assumed to contain 24 pores per µm^2 with an average pore diameter of 0.1 µm. If it is further assumed that the pores are cylindrical and uniform throughout, then a film surface area of 8.8 m^2/g is obtained. For an etching rate of 4.0 µm/min, a surface reaction rate of 1.9×10^{19} UF_6 molecules/m^2 s is calculated from Eq. (1). This reaction rate compares favorably with other actinide etching studies. For example, a rate of 1.9×10^{17} PuF_6 molecules/m^2 s was reported for the removal of PuO_2 films with a low-pressure CF_4/O$_2$ plasma [3].

We have previously examined the gas-phase chemistry of the CF_4-based atmospheric pressure plasma in order to better understand the metal etching process [14]. In particular, the concentration of fluorine atoms downstream of the discharge was measured by hydrogen titration. It was found that the F concentration ranges from 10^{21} to 10^{22} m^{-3}, depending on the partial pressure of CF_4 and the input power density. This concentration is roughly two orders of magnitude higher than that found in low-pressure fluorine plasmas [15,16]. The other most abundant reactive species are CF_2 and CF_3. These radicals are rapidly converted to C_2F_6, so that their concentration quickly falls below 10^{18} m^{-3} in the afterglow. The low density of these radicals may explain why no fluorocarbon polymers are deposited on the sample surface during etching. Based on this previous work, it may be concluded that fluorine atoms are the principal reactive species in the downstream region of the atmospheric pressure plasma.

During etching, the surface of the uranium oxide film is quickly converted into uranium oxyfluoride, mainly UOF_4. Evidently, these fluorinated species must build up on the surface before the incoming F atoms can react with it and produce the volatile UF_6 reaction product. This is consistent with previous studies of heavy metal etching. For example, Kim et al. [5] observed the formation of uranium oxyfluorides during the low-pressure plasma etching of UO_2. In addition, we found that tantalum foil surfaces become covered with TaO_xF_y species upon exposure to the atmospheric pressure CF_4/O$_2$/He plasma at 300 °C [11].

Although we do not have enough evidence to make any definite conclusions, it appears that the kinetically slow step in the overall process may be the reaction of gas-phase or adsorbed F atoms with UOF_4 species to desorb UF_6. Machiels and Olander [17] have proposed a similar mechanism for tantalum etching in an F_2 molecular beam, in which the rate-limiting step is the reaction between adsorbed F and a fluorinated surface layer. In this regard, it is interesting to estimate the collision rate of F atoms with the film surface relative to the rate of F atom conversion into UF_6. From kinetic theory, the former rate is estimated to be 1.8×10^{23} molecules/m^2 s for an F atom density of 1×10^{21} m^{-3} above the film surface. On the other hand, Eq. (1) yields an F atom conversion rate into UF_6 of 1.1×10^{20} molecules/m^2 s. These calculations suggest that in the present process, the overall reaction is not limited by the flux of F atoms to the surface.

5. Conclusions

We have studied the etching of uranium oxide films deposited on stainless steel surfaces with a low temperature, atmospheric pressure CF_4/O$_2$/He plasma. An etching rate of 4.0 µm/min was observed at a sample temperature

of 200 °C. These results suggest that atmospheric pressure plasmas are a promising technology for the decommissioning and decontamination of transuranic wastes.

Acknowledgements

References

[1] The US Department of Energy's Environmental Management Science Program, Report DOE-ID-10840, 2001.

[2] The US Department of Energy's Environmental Management Science Program, Annual Report 2000, Report DOE/EM-0569, 2000.

[3] J.C. Martz, D.W. Hess, J.M. Haschke, J.W. Ward, B.F. Flamm, J. Nucl. Mater. 182 (1991) 277.

[4] J.M. Veilleux, M.S. El-Genk, E.P. Chamberlin, C. Munson, J. FitzPatrick, J. Nucl. Mater. 277 (2000) 315.

[5] Y.S. Kim, J.Y. Min, K.K. Bae, M.S. Yang, J. Nucl. Mater. 270 (1999) 253.

[6] H.F. Windarto, T. Matsumoto, H. Akatsuka, M. Suzuki, J. Nucl. Sci. Technol. 37 (2000) 787.

[7] A. Schütze, J.Y. Jeong, S.E. Babayan, J. Park, G.S. Selwyn, R.F. Hicks, IEEE Trans. Plasma Sci. 26 (1998) 1685.

[8] J.Y. Jeong, J. Park, I. Henins, S.E. Babayan, V.J. Tu, G.S. Selwyn, G. Ding, R.F. Hicks, J. Phys. Chem. 104 (2000) 8027.

[9] S.E. Babayan, G. Ding, R.F. Hicks, Plasma Chem. Plasma Process. 21 (2001) 505.

[10] J. Park, I. Heninis, H.W. Herrmann, G.S. Selwyn, R.F. Hicks, J. Appl. Phys. 89 (2001) 20.

[11] V.J. Tu, J.Y. Jeong, A. Schütze, S.E. Babayan, G. Ding, G.S. Selwyn, R.F. Hicks, J. Vac. Sci. Technol. A 18 (2000) 2799.

[12] C.D. Wagner, W.M. Riggs, L.E. Davis, J.F. Moulder, G.E. Muilenberg, Handbook of X-ray Photoelectron Spectroscopy, Perkin–Elmer, 1979.

[13] M. Iwasaki, J. Nucl. Mater. 25 (1968) 216.

[14] X. Yang, S.E. Babayan, R.F. Hicks, Plasma Sources Sci. Technol. 12 (2003) 484.

[15] J.S. Jenq, J. Ding, J.W. Taylor, N. Hershkowitz, Plasma Sources Sci. Technol. 3 (1994) 154.

[16] K. Sasaki, Y. Kawai, C. Suzuki, K. Kadota, J. Appl. Phys. 82 (1997) 5938.

[17] A.J. Machiels, D.R. Orlander, Surf. Sci. 65 (1977) 325.